Journal of Geoscience and Environment Protection, 2025, 13(12), 494-511
https://www.scirp.org/journal/gep
ISSN Online: 2327-4344
ISSN Print: 2327-4336

Relations between Coastal Eutrophication and Sea Foam Formation during a Cold Front Passage. Case Study on Santos City Beaches (Brazilian Subtropical Coast)

Bruno Otero Sutti, Henrique José Rodrigues Dias, Nixon Claudio Sakazaki, Antonio Jeferson Muniz Almeida, Vitor Gonsalez Chiozzini, Glaucia Bueno Benedetti Berbel, Elisabete de Santis Braga

Oceanographic Institute, University of São Paulo, São Paulo, Brazil
Email: edsbraga@usp.br

How to cite this paper: Sutti, B. O., Dias, H. J. R., Sakazaki, N. C., Almeida, A. J. M., Chiozzini, V. G., Berbel, G. B. B., & Braga, E. S. (2025). Relations between Coastal Eutrophication and Sea Foam Formation during a Cold Front Passage. Case Study on Santos City Beaches (Brazilian Subtropical Coast). *Journal of Geoscience and Environment Protection, 13,* 494-511.
https://doi.org/10.4236/gep.2025.1312025

Received: November 25, 2025
Accepted: December 23, 2025
Published: December 26, 2025

Abstract

Sea foams are caused by algal blooms and can represent large areas in coastal waters during ocean fronts associated with meteorological changes that establish rainy weather and high wave incidence. Especially in urban areas along the Brazilian southeast coast, eutrophication has been evidenced as an enhancement factor for this phenomenon. The present study was conducted on Santos City beaches during foam presence, which showed a wide distribution from the surf zone up to urban structures above the high tide limit. Water and foam samples were collected from pluvial canals that connect to Santos Bay to investigate the origin of the foam and the relationship between this phenomenon and eutrophication levels. The eutrophication analysis was based on various species of nutrients (urea, ammonium, nitrite, nitrate, phosphate, and silicate), photo-pigments, and a trophic index. A cold front passage provided intense south winds (>10 m s^{-1}) and high waves (>1 m) before the sampling day. In addition to this storm surge, an accumulated rainfall of ≈ 50 mm and a spring tide condition led to overwash at the floodgates of the pluvial canals. Salinity showed negative correlations with dissolved nutrients, indicating that increased freshwater outflows improved the trophic indices on both sides of the floodgates. At the foam sampling site, elevated concentrations of suspended particulate matter were associated with a high algal content, as primarily indicated by high chlorophyll a within particulate organic matter content. This occurred alongside high oxygen saturation and relatively low nutrient concentrations, suggesting the growth of opportunistic phytoplankton species. Our results suggest that eutrophication can intensify sea foam occurrence during

overwash periods of the floodgates. However, phytoplankton analyses and more sampling sites need to be integrated into further studies for a better understanding of the local eutrophication influence on sea foam formation.

Keywords

Coastal Waters, Sea Foam, Nutrients, Eutrophication, Cold Front

1. Introduction

Foams in coastal waters typically originate from dissolved organic matter (DOM) with surfactant properties (responsible for foam stabilization), especially when agitated mechanically, such as by breaking waves, wind action, and motorized boat movement (Oliveira et al., 2014). A non-surfactant but inherently more viscous liquid, or one rendered more viscous by DOM, will also drain more slowly and thus also stabilize the foam (Jenkinson et al., 2021). When the foam is generated by DOM of autochthonous origin (specifically from algal blooms), it is denominated as "sea foam" or "beach foam" (**Figure 1**) (Outhward, 1953). In general, the major components of DOM in seawater are, in order of abundance, carbohydrates, proteins, and lipids (Hansell & Carlson, 2002), while sea foams tend to concentrate these constituents, as well as products of phytoplankton activities (e.g., chlorophylls and phaeopigments). In New Brunswick (Canada), sea foam samples revealed phenolic compounds, carbohydrates, amino acids, and proteins accounting for 25% - 90% of the total soluble organic carbon (Bärlocher et al., 1988). In this sense, sea foams can establish an ephemeral hotspot for distinctive bacterial communities (Rahlff et al., 2021).

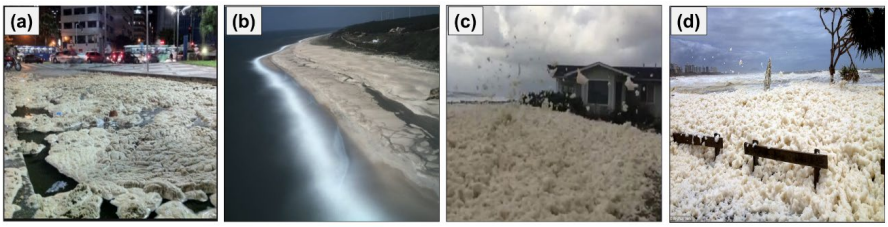

Figure 1. Beach foam occurrence around the world. (a) Santos City (Authors); (b) Nazaré (Portugal) (Oliveira et al., 2014); (c) Oregon (Estados Unidos) (Mail Online, 2018); (d) Queensland (Austrália) (Mail Online, 2018).

In coastal regions of the Northern Sea, large areas of sea foam have been observed during occurrences of ocean fronts in cases when meteorological changes established rainy weather (i.e., intensifying nutrient inputs) and high wave incidence (i.e., under strong winds), thus providing ideal conditions for the development of specific phytoplankton groups and foam formation, respectively (Baumann et al., 1994; Gypens et al., 2007; Blauw et al., 2010). In Brazil, this phenomenon has been more frequently observed along the southern and southeastern

coasts, where cold fronts occur with higher frequency and intensity. Especially in urban areas along the São Paulo coast (Brazilian southeastern coast), these episodes have caused concern among the population since environmental management departments face difficulties in accurately informing the cause of this phenomenon. Such difficulties refer to existing gaps involving a synergistic association with coastal eutrophication. In Europe's coastal waters, eutrophication has promoted harmful algal blooms associated with water discoloration and foam formation (Aertbjerg et al., 2001).

In this context, a deep investigation of coastal eutrophication during ocean front influence is essential to verify whether these phenomena are related to biogeochemical drivers of sea foam formation. First, it is crucial to recognize the differences between anthropogenic nutrient inputs and biogeochemical signatures of water mass associated with the ocean front, as well as which Nitrogen (N), Phosphorus (P), and Silicon (Si) levels are triggering phytoplankton blooms (e.g., concerning high chlorophyll-a concentrations) in the adjacent sea. In addition to N:P:Si ratios, An and Du (2000) found a consistent relation between chlorophyll ratios (a:b:c) and the quantitative distribution of the main phytoplankton groups in a large subtropical coastal area in Asia.

The present study was conducted on Santos City beaches during foam presence, which showed wide distribution from the surf zone up to urban structures above the high tide limit (**Figure 1(a)**). Water and foam samples were taken from pluvial canals that connect with the adjacent sea (Santos Bay) to investigate the origin of foam and the relations between this phenomenon and the eutrophication level. The eutrophication analysis was based on various species of nutrients (urea, ammonium, nitrite, nitrate, phosphate, and silicate), N:P:Si ratios, photo-pigments, and trophic index (TRIX). Additionally, meteorological and oceanographic variables were reported during the sampling period to verify ocean front passage.

2. Material and Methods

2.1. Study Area and Sampling Strategy

Santos City is located in the southeastern Brazilian coast (more exactly in the central littoral of São Paulo state) along an area of climate transition (from Atlantic tropical to humid subtropical climes), within which polar masses are prevalent in winter and tropical ones in summer. The proximity of the Serra do Mar ridge, associated with high evaporation rates (usually in summer days) and the influence of cold fronts (more intense and long-lasting in winter), provides high average annual rainfall, between 2000 and 3000 mm (Nunes, 1990). Besides, the region has evidenced a higher occurrence of extreme events, which refers to bulky daily rainfall (commonly in summer) (Zilli et al., 2016) and storm surges (commonly in winter) (Campos et al., 2010).

Santos is the most important and populous city on the São Paulo coast, in which the port, industrial, and tourist sectors represent a substantial contribution to the Brazilian GDP (Gross Domestic Product). Consequently, Santos Bay may receive

wastewater from point and diffuse sources of several anthropogenic activities, mainly through the port channel and seven pluvial canals (Figure 2). Such entrances were pointed out as strong drivers of eutrophication processes in Santos Bay (Braga et al., 2000; Moser et al., 2005; Berbel et al., 2015).

Figure 2. (a) Santos City localization and its integrated system of freshwater runoff capitation. The network of pluvial canals is shown in red, highlighting the sampling locations in canals 1, 3, and 6. In blue, it shows the integration between pluvial canals and the sewage treatment system, where the water flow is directed to the Sewage Preconditioning Station (EPC) and, subsequently, released by the submarine outfall. Details of the external (b) and internal (c) sides of an operating gate.

Posteriorly to the floodgate system installation (in 1992), water exchanges between Santos Bay and pluvial canals were minimized, thereby increasing the efficiency of freshwater runoff capture and its conduction toward the EPC (Sewage Preconditioning Station). However, the pluvial canals are not the main system of waste; they represent a pluvial system that sometimes contains impurities from the city drainage. As a result, on occasions of high flow, it is conducted through the submarine outfall and released approximately 4.5 km from the coast (Coelho et al., 2012). Despite that, striking meteorological tides associated with cold fronts have exceeded the height of the gates, causing a pluvial and seawater mix.

In this context, a campaign was performed on October 24, 2017, to obtain water samples from the inner and outer sides of gates 1, 3, and 6 during a foam occurrence period (Figure 2). Meanwhile, a foam sample was acquired in an area close

to the sampling site on the inner side of Canal 1. It is important to note that the floodgates usually operate closed during periods of high rainfall and waves, as was the case these days under the influence of the cold front, including the sampling day. Finally, the same variables were obtained from both samples (water and foam).

2.2. Metocean Data

The dataset of the National Institute of Meteorology (INMET, 2019) was consulted to obtain meteorological parameters. The institute operates a meteorological station in Santos City, from which monthly and daily rainfall indexes were acquired, as well as hourly measurements of air temperature, radiation, atmospheric pressure, and wind speed during the sampling day. In turn, the tidal conditions during the sampling day were obtained from the Brazilian Navy Directory (DHN, 2019).

2.3. Analytical Determination from Water Samples

Water temperature was measured directly in the pluvial canals by portrait thermometer. Surface waters were collected by van Dorn bottles to attempt the analytical determinations in the laboratory. Immediately after sampling, DO was determined according to the Winkler method (Grasshoff et al., 1983), whereas the dissolved oxygen saturation (DO%) was calculated through equations proposed by Aminot and Chaussepied (1983). The pH values were measured through the Orion® pH-meter (precision of 0.001) (Grasshoff et al., 1983). The salinity was determined through an inductive salinometer (Beckman®) following the equations in Fofonoff & Millard (1983). Suspended Particulate Matter (SPM) was determined by the gravimetric method, while Particulate Organic Matter (POM) was established after volatilization in a muffle furnace (Strickland & Parsons, 1968).

Photo-pigment and nutrient analysis were performed by the spectrophotometric method. The chlorophyll determination followed the methods of Jeffrey and Humphrey (1975) and Lorenzen (1965) concerning the determinations of chlorophylls (a, b, and c) and phaeopigments, respectively. Dissolved nutrients were analyzed by colorimetric methods with precisions of 0.01 μmol L^{-1}. Inorganic phosphorus (DIP) and silicon (DSi) were analyzed according to Grasshoff et al. (1983). Ammonium ($N\text{-}NH_4^+$) was determined following Tréguer & Le Corre (1975), while nitrate ($N\text{-}NO_3^-$) and nitrite ($N\text{-}NO_2^-$) were measured using an AutoAnalyzer II (BranLuebbe®) according to Grasshoff et al. (1983). Dissolved Inorganic Nitrogen (DIN) was calculated as the sum of NH_4^+, NO_2^-, and NO_3^-. In turn, the urea content was analyzed following Aminot & Kerouel (1982).

The present work adopted the TRIX equation proposed by Vollenweider et al. (1998) for Mediterranean coastal waters, as follows:

$$TRIX = [\log 10\,(DIP * DIN * Chla * dDO\%) + a]/b \quad (1)$$

in which: *dDO*% is the absolute deviation of dissolved oxygen saturation; and *a* (1.5) and *b* (1.2) are scale coefficients.

The coefficients (a) and (b) were proposed by Giovanardi and Vollenweider (2004) to establish a scale ranging from 0 to 10 (**Table 1**). However, studies on eutrophication processes in Brazilian coastal environments (Cotovicz-Junior et al., 2012; Santos et al., 2021) report that the TRIX indexes are more representative for the trophic state of tropical and subtropical waters on reduced scales, in which the poorer conditions are better characterized below 10. Considering two annual periods (2021-2023) and six sampling sites in the Rushikulya estuary (India), Gogoi et al. (2024) observed that the TRIX values underestimated the local eutrophication. Despite the causes of these differences not being understood, the authors mention the distinct climatic conditions as the main conditioning factor. Thus, we adopted the adaptation proposed by Silva et al. (2025), which modifies the scale to range from 0 to 6.

Table 1. Trophic State Classification for estuarine waters according to the TRIX Model (adapted from Giovanardi & Vollenweider, 2004).

TRIX	Water Conditions	Trophic State
<2	Very poorly productive and very low trophic state	Excellent (Ultraoligotrophic)
2 - 4	Poorly productive and low trophic state	Good (Oligotrophic)
4 - 5	Moderately productive and of medium trophic state	Moderate (Mesotrophic)
5 - 6	Highly productive and high trophic state	Poor (Eutrophic)
>6	Highly productive and highest trophic state	Very poor (Hypereutrophic)

2.4. Statistic Treatment

Descriptive and multivariate statistics were performed in GraphPad Prism®. The concentrations of nutrients (DSi + DIN + DIP), nitrogen forms (nitrate + nitrite + ammonium + urea), suspended particulate matter (POM + PIM), and photopigments (chlorophylls a, b, c, and phaeopigments) were expressed in stacked bar charts. The Shapiro-Wilk analysis tested the normality of the data. Finally, the Spearman correlation and analyses of principal component (PCA) and clustering were conducted to verify the physical and biogeochemical relations between foam and water samples.

3. Results and Discussion

3.1. Meteorological and Oceanographic Conditions

Meteorological variables reported per hour over nine days before the sampling are presented in **Figure 3**. Atmospheric pressure higher than 1015 mb under mild temperatures (20˚C - 25˚C) and winds coming from the north quadrant characterized a period of meteorological stability from 15 to 17 October. Subsequently, on days 18 - 19th, a reduction in atmospheric pressure was associated with an increase in radiation, temperature, and wind speed (NW), thereby configuring a

pre-frontal system. On the 20th, a cold front reached Santos City under winds from the south quadrant, followed by a gradual decrease in temperature until the sampling day (24th).

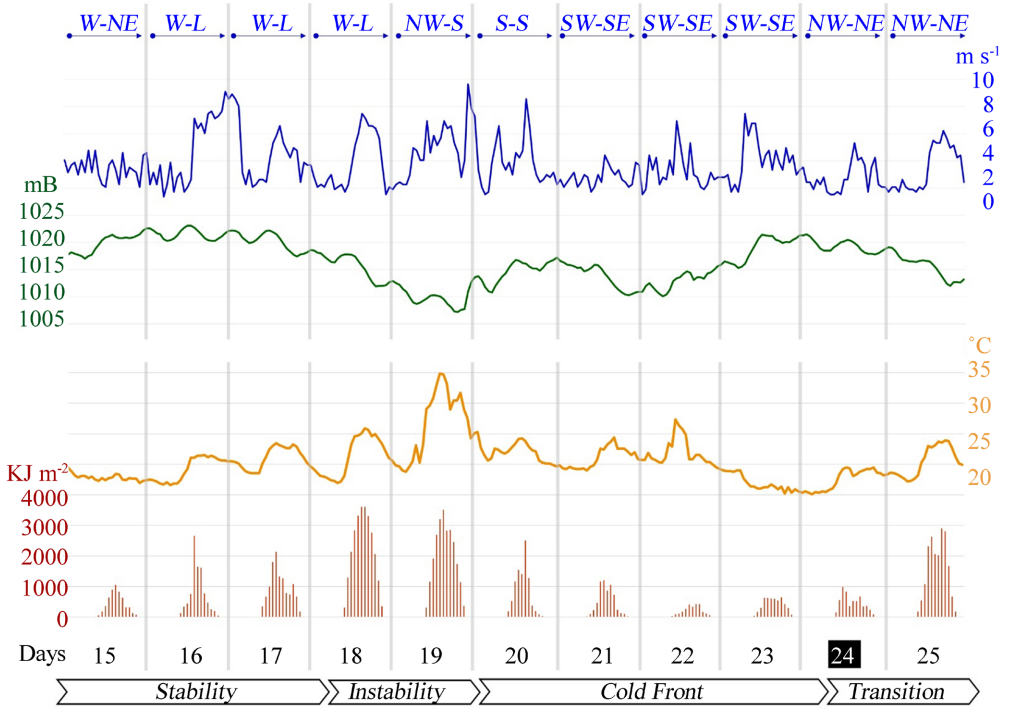

Figure 3. Meteorological variables reported per hour (INMET, 2019). In blue, wind speed and prevailing directions. In green, atmospheric pressure in millibars (mb). In orange, air temperature. In red, radiation in kilojoules per square meter (KJ m^{-2}). Note: The sampling day is highlighted in the black box, and the flowchart indicates shifts in meteorological conditions.

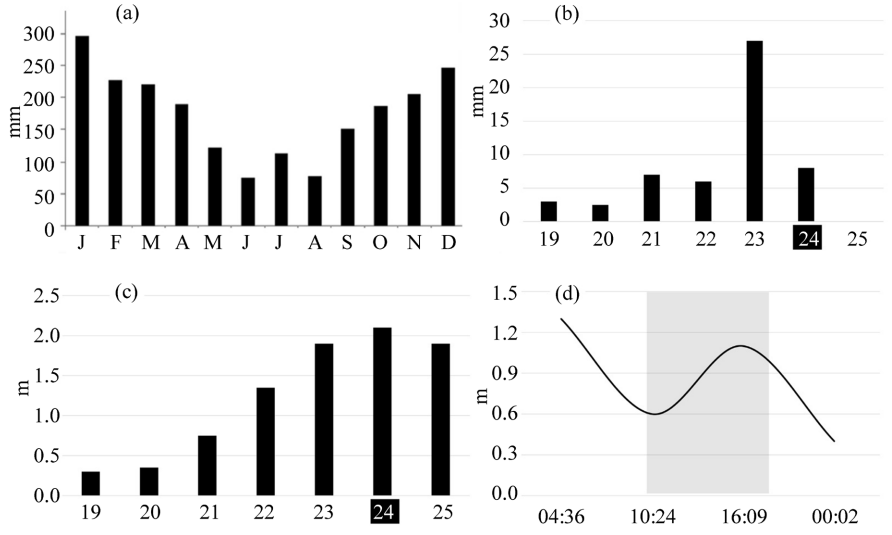

Figure 4. (a) Monthly rainfall of 2017; (b) Rainfall (accumulated) relative to 5 days before the sampling day; (c) Average daily wave size (from 19 to 25 October/2017); (d) Tidal curve relative to the sampling day, highlighting the sampling period (10:00 - 16:30).

The annual standard of the regional rainfall can be observed through the average monthly indices obtained from a series of 60 years, shown in **Figure 4(a)**. According to **Figure 4(b)**, it is possible to infer that the cold front passage promoted a rainy period until the sampling day, highlighting the accumulated volume on day 23rd (≈28 mm). Besides, the cold front passage, under winds coming from the south, favored the incidence of relatively high waves into Santos Bay, with a peak on the sampling day (> 2.0 m) (**Figure 4(c)**, **Figure 4(d)**), in turn, shows that the sampling period on the 24th happened during the ascent of a spring tide, which, in synergy with the high wave energy, provided a striking sea level rise.

3.2. Physical and Biogeochemical Variables

3.2.1. Physicochemical Properties

Water temperature practically did not vary between the canal sides, as well as between the water and foam samples. The foam sample was taken from the internal side of canal 1 (I-1), but its physical and chemical properties (salinity, pH, and DO) were closer to the external sides of canals 1 (E-1) and 6 (E-6). In relation to the external side (E) of the canals, the water samples taken from the internal side (I) showed lower values in Secchi disc depth, salinity, pH, and dissolved oxygen (DO) (**Table 2**). High oxygen saturations (DO% > 80%) were found in canals 1 and 6, whereas hypoxic conditions (DO% < 50%) were evidenced in canal 3. According to Breitburg (2002), hypoxic conditions in coastal waters are favored under DO% values below 50%.

Table 2. Physical and chemical water properties in the internal (I) and external (E) part of the pluvial canals at Santos coast in October 2017.

Canals	Secchi D. (cm)		Temp. (°C)		Salinity		pH		DO (mL L^{-1})		DO%	
	I	E	I	E	I	E	I	E	I	E	I	E
1	80	20	23.3	23.1	20.1	34.7	7.9	8.1	5.4	6.3	101	128
3	70	15	23.5	22.9	10.6	16.9	7.5	7.6	1.7	2.9	30	55
6	60	30	23.3	23.4	15.5	24.3	7.7	8.0	4.5	5.8	82	113
Foam (C1)	---		23.2		28.6		8.1		6.3		130	

3.2.2. Dissolved Nutrients (N, P, and Si)

In general, the lowest dissolved nutrient concentrations were found in the E-1 and foam, while the highest ones were found in the I-3 and I-6 (**Figure 5**). The concentrations of inorganic dissolved silicate (DSi) varied from 7.62 μmol L^{-1} (E-1) to 112.58 μmol L^{-1} (I-6), Dissolved Inorganic Nitrogen (DIN) from 5.92 μmol L^{-1} (E-1) to 59.54 μmol L^{-1} (I-6), and Dissolved Inorganic Phosphorus (DIP) from 1.24 μmol L^{-1} (Foam) to 6.90 μmol L^{-1} (I-3) (**Figure 5(a)**). Concerning the N-forms (**Figure 5(b)**), ranges of 4.06 - 4 7.71 μmol L^{-1} for NO_3^-, 1.20 - 11.15 μmol L^{-1} for NH_4^+, and 0.71 - 5.58 μmol L^{-1} for NO_2^-, while 4.36 - 25.79 μmol L^{-1} for urea, an organic component, were observed, configuring in all sampling sites the

following composition: NO_3^- > urea > NH_4^+ > NO_2^-. Thus, NO_3^- was the main nutrient to drive the trophic indexes, which revealed hypereutrophic conditions in I-3 and E-3, eutrophic in I-6 and foam, mesotrophic in E-6 and I-1, and oligotrophic in E-1 (Figure 5(c)). The organic N form available, urea, is also representative of an anthropogenic source.

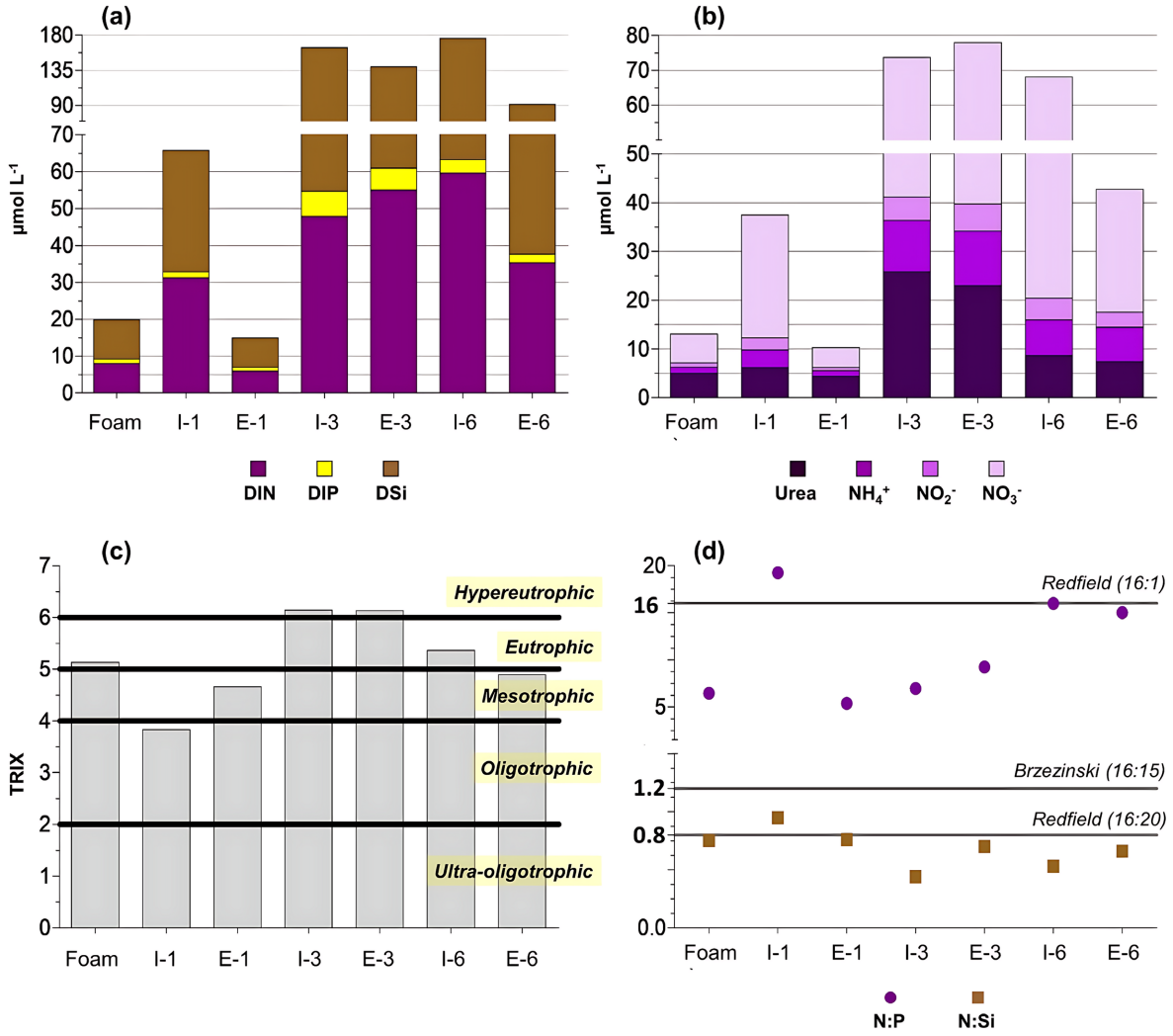

Figure 5. (a) Dissolved inorganic nutrients in the bar chart: nitrogen (DIN), phosphorus (DIP), and silicate (DSi); (b) Dissolved nitrogen forms in the bar chart: urea, ammonium (NH_4^+), nitrite (NO_2^-), and nitrate (NO_3^-); (c) Trophic Indexes (TRIX); (d) N:P:Si ratios of marine organic matter established by Redfield et al. (1963) (16:1:20) and Brzezinski (1985) (16:1:15).

Finally, N:P:Si ratios are shown in Figure 5. The N:P:Si ratio of POM (phytoplankton) most used in marine biogeochemical studies is the Redfield (1958) (16:1:20). Subsequently, Brzezinski (1985) observed that an N:P:Si ratio of 16:1:15 provided ideal growth conditions for 27 species of diatom, of which 18 (> 20 µm) showed a slightly higher mean N:Si ratio (1.2). However, depending on the physical-biogeochemical conditions of the water column, deviations from these ratios

can be significant, mainly concerning the temperature and trophic status (i.e., under depleted or rich nutrient conditions) (Sharoni & Halevy, 2020). In most sampling sites, N:P:Si ratios remained below the ratio of 16:1:15 and 20:1:16, suggesting that no basic element of the habitat indicated nutrient limitation (**Figure 5(d)**). The exception was observed at I-1, where the Redfield ratios suggested a limitation both for DIP (N:P > 16) and DSi (N:Si > 0.8).

3.2.3. Suspended Particulate Matter and Photopigments

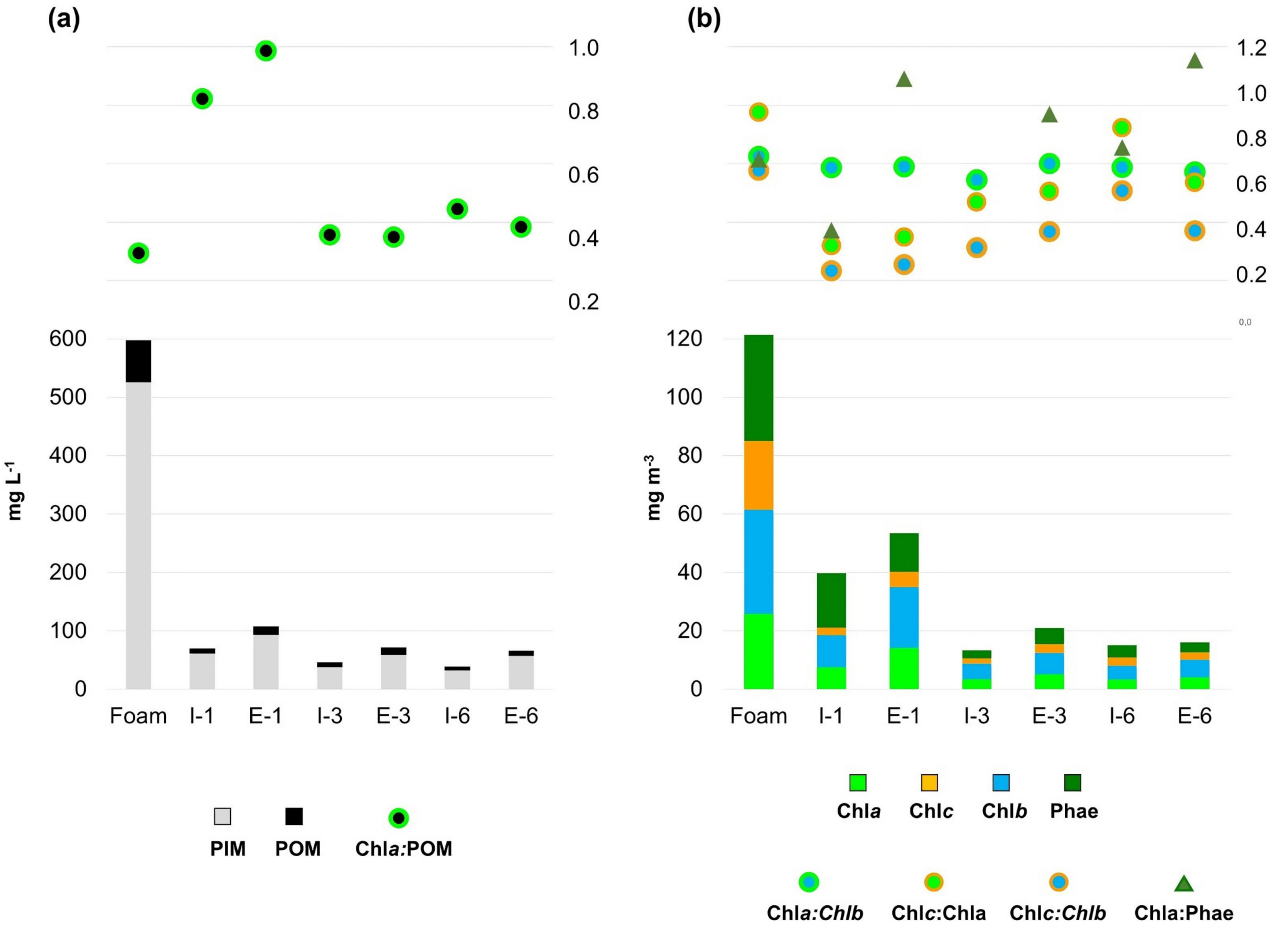

Figure 6. (a) Suspended particulate matter (POM + PIM) concentrations in the bar chart, and Chla:POM ratio in line points; (b) Chlorophylls (a, b, and c) and phaeopigment (Phae) concentrations in the bar chart, and pigment ratios in line points.

Concentration ranges of POM (Particulate Organic Matter) and PIM (Particulate Inorganic Matter) reached 6.57 - 14.29 and 32.29 - 93.43 mg L^{-1} in water samples, respectively (**Figure 6(a)**). Meanwhile, the foam sample displayed concentrations considerably higher, both in POM (72.01 mgL^{-1}) and PIM (526.08 mgL^{-1}). In coastal waters, POM includes living organisms (such as phytoplankton, bacteria, and protozoa) and particulate detritus, while the PIM, which is primarily constituted of mineral particles, may also be represented by a high proportion of diatom frustules (Kostadinov et al., 2012; Zhang et al., 2014). Within the POM pool, Chla indicates the algal content of samples because it rapidly degrades outside living

cells and comprises a negligible fraction of detrital organic carbon (mainly in oxic waters) (Furlong & Carpenter, 1988). For this reason, the Chla:POM ratio is an efficient means of indicating algae association (mainly regarding the fine fraction of POM) (Hamilton et al., 2005). The lowest Chla:POM ratio was observed in the foam sample and the highest at the E-1 site.

Chlorophylls (a, b, and c) and phaeopigment (Phae) concentrations and their ratios are shown in **Figure 6(b)**. Water samples showed the following ranges of pigment concentration (mg m^{-3}): 3.38-14.12 for Chla, 4.82 - 20.84 for Chlb, 1.77 - 5.24 for Chlc, and 2.77 - 18.64 for Phae. The use of chlorophylls a, b, and c (determined by spectrophotometry) has provided reasonable distinctions among the main phytoplankton groups relative to their ratios, as follows: Chla:Chlb of 0.43 ± 0.22 for green algae, Chlc:Chla of 0.62 ± 0.13 for Diatoms, Chlc:Chla of 0.86 ± 0.56 for Dinoflagellates, and Chlc:Chla of 0.51 ± 0.24 for Cryptophyceae (Cirenko, 1980; An & Du, 2000). Chlorophylls a, b, and c provided reasonable distinctions among the main phytoplankton groups relative to their ratios, as follows: Chla:Chlb of 0.43 ± 0.22 for green algae, Chlc:Chla of 0.62 ± 0.13 for Diatoms, Chlc:Chla of 0.86 ± 0.56 for Dinoflagellates, and Chlc:Chla of 0.51 ± 0.24 for Cryptophyceae (Cirenko, 1980; An & Du, 2000). Considering the ratios observed in the water samples, the Chla:Chlb showed low variation (0.65 - 0.69), Chlc:Chla varied from 0.33 (I-1) to 0.85 (I-6), Chlc:Chlb varied from 0.22 (I-1) to 0.57 (I-6), and Chla:Phae varied from 0.40 (I-1) to 1.22 (I-3). In turn, the seafoam sample showed Chla:Chlb, Chlc:Chla, Chlc:Chlb and Chla:Phae ratios of 0.72, 0.92, 0.66 and 0.71, respectively.

3.2.4. Data Integration

Salinity showed significant correlations with most biogeochemical variables (**Figure 7**), correlating negatively with dissolved nutrients (DSi, DIP, Urea, NH_4^+, NO_3^-, and NO_2^-), and positively with suspended particulate matter (POM and PIM) and chlorophylls (*a* and *b*). It is also important to highlight the positive correlations involving suspended particulate matter with chlorophylls and phaeopigment, and the negative ones involving oxygen saturation (DO%) with dissolved nutrients.

	Sal	Chla	Chlb	Chlc	Phae	pH	DO%	NH_4^+	NO_2^-	NO_3^-	Urea	DIP	DSi	PIM	POM
Sal															
Chla	**0.821**														
Chlb	**0.821**	**0.999**													
Chlc	0.571	0.536	0.536												
Phae	0.643	**0.857**	**0.857**	0.464											
pH	**0.929**	0.750	0.750	0.571	0.679										
DO%	**0.929**	0.750	0.750	0.571	0.679	**0.999**									
NH_4^+	**-0.857**	-0.714	-0.714	-0.357	-0.643	**-0.893**	**-0.893**								
NO_2^-	**-0.857**	-0.714	-0.714	-0.357	-0.643	**-0.893**	**-0.893**	**0.999**							
NO_3^-	**-0.883**	**-0.829**	**-0.829**	-0.360	-0.541	**-0.811**	**-0.811**	**0.883**	**0.883**						
Urea	**-0.929**	**-0.786**	**-0.786**	-0.464	-0.750	**-0.929**	**-0.929**	**0.964**	**0.964**	**0.847**					
DIP	**-0.929**	**-0.786**	**-0.786**	-0.464	-0.750	**-0.929**	**-0.929**	**0.964**	**0.964**	**0.847**	**0.999**				
DSi	**-0.929**	**-0.929**	**-0.929**	-0.429	-0.714	**-0.821**	**-0.821**	**0.857**	**0.857**	**0.955**	**0.893**	**0.893**			
PIM	**0.821**	**0.999**	**0.999**	0.536	**0.857**	0.750	0.750	-0.714	-0.714	**-0.829**	**-0.786**	**-0.786**	**-0.929**		
POM	**0.821**	**0.893**	**0.893**	0.750	0.643	0.714	0.714	-0.536	-0.536	-0.739	-0.643	-0.643	**-0.821**	**0.893**	

p < 0.05

Figure 7. Pearson correlation.

The cluster analysis clearly separated the sampling sites by importance in nutrients and SPM/pigments, reflecting the higher nutrient levels and trophic indexes at pluvial canals 1 and 3, and the higher SPM and pigment concentrations at canal 1 (including the sampling site of foam) (Figure 8).

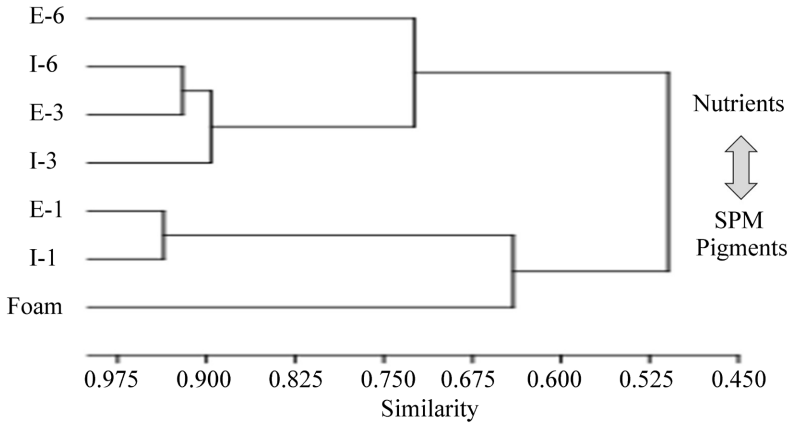

Figure 8. Cluster analysis.

4. Discussion

The meteorological and oceanographic conditions set a cold front passage that extended from 20 to 26 October 2017, coinciding with this study's sampling period. Such conditions corroborate previous meteorological analyses (at mesoscale) along the Brazilian south and southeast coasts (Harari et al., 2008; Seluchi et al., 2017), which displayed an atmospheric pressure fall associated with wind rotation from northwest to south, followed by a sharp air temperature decrease. Consequently, south winds provided waves of up to 2 m in Santos Bay, reaching 1 m during the sampling day. In addition to wind and wave forces, the spring tide during the flooding phase contributed to the high presence of foam on urban structures above the high-tide limit.

Changes in meteorological conditions led to relatively rainy days, mainly on 23 October (before the sampling day), thereby triggering an increase in freshwater discharges into Santos Bay. Despite the considerable salinity differences observed between the sides of the floodgates, the inner sides revealed relatively high values, indicating overwash events during the cold front passage and, consequently, a water mixture between pluvial canals and Santos Bay. In inner areas of the São Paulo continental shelf, there is a predominance of the coastal water mass—CW (temperature > 21˚C and salinity ~34.5) in surface layers during most of the year, while the formation of the south coastal water mass—SCW (temperature 18 - 21˚C and salinity < 34) occurs during cold fronts (mainly in wintertime) due to mixing processes and seasonal cooling (Silva et al., 2001). In the present study, a water temperature range of 22.9 - 23.5˚C reflected the mix of continental and coastal waters.

The negative correlations between salinity and dissolved nutrients indicate the intensification of continental inputs during rainy periods. Compared to dry peri-

ods, the port estuarine channel can considerably increase nutrient export (>50%) to Santos Bay after rainy events, primarily in SiD, NH_4^+, and NO_3^-, thereby making a significant contribution to coastal eutrophication (Braga et al., 2000; Moser et al., 2005; Masuda et al., 2011). Concerning the pluvial canals, the present study observed similar values to Braga et al. (2000), which showed accentuated differences in nutrient concentrations (NH_4^+, NO_3^-, and PO_4^{3-}) between inside (≈40.0, 42.0, and 4.0 μmol L^{-1}) and outside (10.0, 11.0, and 1.5 μmol L^{-1}) of the floodgates. Besides, the authors concluded that the pluvial canals represent an important contribution of heterotrophic bacteria (*Escherichia coli*) to the Santos beaches. Particularly at canal 3, we observed low variation in salinity (10.6 - 16.9), pH (7.5 - 7.6), dissolved oxygen (1.7 - 2.9 mL L^{-1}), and trophic status (TRIX > 6) between inside and outside of the floodgate, evincing that overwashes during cold fronts can modify the metabolism (from autotrophic to heterotrophic) in the Santos Bay.

Overall, the cluster analysis showed two different biogeochemical conditions. At canals 3 and 6, the higher trophic indexes showed a substantial contribution of DIN and a low contribution of Chla, thereby suggesting advanced stages of eutrophication despite the high oxygen saturation (DO%) observed at E-6. Meanwhile, at canal 1, where the foam sample was taken, high SPM concentrations associated with high algal content (indicated primarily by high Chla:POM ratios) under high DO% values and relatively low nutrient concentrations suggested the development of opportunistic phytoplankton species. Moreover, the positive correlations involving salinity with SPM and chlorophylls strongly point out the phenomenon of sea foam.

In the foam sample, high phaeopigment (Phae) concentrations and a lower Chla:POM ratio indicated decreased photosynthetic activity relative to the surrounding water body (i.e., I-1 and E-1 sampling sites), probably due to the high SPM concentration (enhanced by the high foam presence) that acted as a limiting factor. Concerning the phytoplankton size, studies in aquatic systems suggest that particles with Chla:POM ratios > 3 can be related to large phytoplankton cells with high sinking potential (Yacobi & Ostrovsky, 2008; Sutti et al., 2023), while the present study revealed considerably lower ratios (0.3 - 1.1). Coastal eutrophication is linked to a shift in phytoplankton from larger, less competitive species to smaller, fast-growing species like diatoms and dinoflagellates, especially opportunistic species (Oviatt et al., 1989; Kimor, 1992).

Changes in phytoplankton composition as a function of tides, wind-induced mixing conditions, and freshwater outflows have been observed in the port estuarine channel and Santos Bay (Masuda et al., 2011; Moser et al., 2012). According to the authors, diatoms are abundant in Santos Bay during high surf zone energies (under strong south winds) and can represent large cells during spring tides after periods of high precipitation rates, while mixotrophic dinoflagellates are enhanced after intense estuarine discharges due to an increase in N-forms (mainly NH_4^+) and a decrease in N:Si ratios. These phytoplankton dynamics occurred in

physical (wind, tide, and rainfall) and biogeochemical (nutrient concentration and composition) conditions similar to those observed in the present study, thereby suggesting that both diatoms and dinoflagellates may have been important to sea foam formation.

In the Northern European coast, massive Phaeocystis spp blooms are the main drivers of large areas of sea foam, which are usually associated with ocean fronts (Gypens et al., 2007; Blauw et al., 2010). Despite this group being favored by nutrient inputs during rainy periods, neither study exhibited evidence of links to coastal eutrophication; probably because it shows a wide variety of marine environments and is rarely stimulated by anthropogenic eutrophication (Baumann et al., 1994; Phaeocystis Research, 2018). Just like Phaeocystis blooms, blooms of diatoms and dinoflagellates can establish gelatinous colonies that are maintained by a mucus-like substance (exopolymeric substances), and when massive blooms die off, the decaying organic material forms a sticky and long-lasting foam (Cuvelier et al., 2010). In the present study, the high Phae concentration in the foam sample suggests that the phytoplankton senescence released the foam-stabilizing dissolved organic matter. In samples taken at the pluvial canals, the high variability in chlorophyll ratios also indicates the presence of both diatoms and dinoflagellates. However, the sea foam sample displayed a Chlc:Chla ratio (0.92) with a higher potential for dinoflagellates.

5. Conclusion

A cold front passage was characterized in Santos city from 20 to 26 October 2017, providing intense south winds (>10 m s^{-1}) and high waves (>1 m) before the sampling day. In addition to this storm surge, an accumulated rainfall of ≈50 mm and a spring tide condition provided overwash periods on the floodgates of the pluvial canals, as indicated by high salinities observed on the inner sides. Salinity showed negative correlations with dissolved nutrients, indicating that increased freshwater outflows increased the trophic indices on both sides of the floodgates.

At the foam sampling site, elevated concentrations of suspended particulate matter (SPM) were associated with a high algal content, as primarily indicated by high chlorophyll a to particulate organic matter (Chla:POM) ratios. This occurred alongside high oxygen saturation (DO%) and relatively low nutrient concentrations, suggesting the growth of opportunistic phytoplankton species. The results from the foam sample support this hypothesis and even imply that opportunistic species produced the viscous substances necessary for foam formation. Furthermore, the positive correlations between salinity and chlorophylls strongly indicate the phenomenon of sea foam.

Our results indicated that the occurrence of this phenomenon on the beaches of Santos is related to the following meteocean factors: passage of cold fronts, influence of continental drainage, and incidence of waves exceeding 1.0 m. Besides, the present study suggested that eutrophication can intensify sea foam occurrence during overwash periods of the floodgates. However, phytoplankton analyses and

more sampling sites (including the Santos Bay) need to be integrated into further studies for a better understanding of the local eutrophication influence on sea foam formation.

Acknowledgement

The authors would like to thank CNPq Proc.308916//2022-0 for the financial support and the collaboration of Giovanna N. Basile.

Conflicts of Interest

The authors declare no conflicts of interest regarding the publication of this paper.

References

Aertbjerg, G., Carstensen, J., Dahl, K., Hansen, J., Nyaard, K., Rygg, B., Sorensen, K., Severinsen, G., Casartelli, S., Achrimpf, W., Schiller, C., & Druon, J. N. (2001). *Eutrophication in Europe's Coastal Waters*. EEA Project Manager: Kunitez, A. Topic Report 7/2001.

Aminot, A., & Chaussepied, M. (1983). *Manuel des anlyses en millieu marin* (395 p.). CNEXO.

Aminot, A., & Kerouel, R. (1982). Dosage automatique de l'urée dans l'eau de mer: Une méthode très sensible à la diacétylmonoxime. *Canadian Journal of Fisheries and Aquatic Sciences, 39,* 174-183. https://doi.org/10.1139/f82-020

An, N. T., & Du, H. T. (2000). Studies on Phytoplankton Pigments: Chlorophyll, Total Carotenoids and Degradation Products in Vietnamese Waters. In *Proceeding of the SEAFDEC Seminar on Fishery Resources in the South China Sea Area IV: Vietnamese Water* (pp. 1-18). Southeast Asian Fisheries Development Center.

Bärlocher, F., Gordon, J., & Ireland, R. J. (1988). Organic Composition of Seafoam and Its Digestion by Corophium Volutator (Pallas). *Journal of Experimental Marine Biology and Ecology, 115,* 179-186. https://doi.org/10.1016/0022-0981(88)90102-5

Baumann, M. E. M., Lancelot, C., Brandini, F. P., Sakshaug, E., & John, D. M. (1994). The Taxonomic Identity of the Cosmopolitan Prymnesiophyte Phaeocystis: A Morphological and Ecophysiological Approach. *Journal of Marine Systems, 5,* 5-22. https://doi.org/10.1016/0924-7963(94)90013-2

Berbel, G. B. B., Favaro, D. I. T., & Braga, E. S. (2015). Impact of Harbour, Industry and Sewage on the Phosphorus Geochemistry of a Subtropical Estuary in Brazil. *Marine Pollution Bulletin, 93,* 44-52. https://doi.org/10.1016/j.marpolbul.2015.02.016

Blauw, A. N., Los, F. J., Huisman, J., & Peperzak, L. (2010). Nuisance Foam Events and Phaeocystis Globosa Blooms in Dutch Coastal Waters Analyzed with Fuzzy Logic. *Journal of Marine Systems, 83,* 115-126. https://doi.org/10.1016/j.jmarsys.2010.05.003

Braga, E. S., Bonetti, C. V. D. H., Burone, L., & Bonetti Filho, J. (2000). Eutrophication and Bacterial Pollution Caused by Industrial and Domestic Wastes at the Baixada Santista Estuarine System—Brazil. *Marine Pollution Bulletin, 40,* 165-173. https://doi.org/10.1016/s0025-326x(99)00199-x

Breitburg, D. (2002). Effects of Hypoxia, and the Balance between Hypoxia and Enrichment, on Coastal Fishes and Fisheries. *Estuaries, 25,* 767-781. https://doi.org/10.1007/bf02804904

Brzezinski, M. A. (1985). The Si:C:N Ratio of Marine Diatoms: Interspecific Variability and the Effect of Some Environmental Variables. *Journal of Phycology, 21,* 347-357.

https://doi.org/10.1111/j.0022-3646.1985.00347.x

Campos, R. M., Camargo, R. D., & Harari, J. (2010). Caracterização de eventos extremos do nível do mar em Santos e sua correspondência com as reanálises do modelo do NCEP no sudoeste do Atlântico Sul. *Revista Brasileira de Meteorologia, 25,* 175-184. https://doi.org/10.1590/s0102-77862010000200003

Cirenko, L. A. (1980). The Information Value of Chlorophyll Index. *Hydrobiological, 4,* 49-53.

Coelho, F. R., Santos, A. R., Cortez, F. S., Pusceddu, F. H., Toma, W., & Guimarães, L. L. (2012). Caracterização da qualidade das águas dos canais de Santos (São Paulo, Brasil). *Unisanta BioScience, 1,* 54-59.

Cotovicz Junior, L. C., Brandini, N., Knoppers, B. A., Mizerkowski, B. D., Sterza, J. M., Ovalle, A. R. C. et al. (2012). Assessment of the Trophic Status of Four Coastal Lagoons and One Estuarine Delta, Eastern Brazil. *Environmental Monitoring and Assessment, 185,* 3297-3311. https://doi.org/10.1007/s10661-012-2791-x

Cuvelier, M. L., Allen, A. E., Monier, A., McCrow, J. P., Messié, M., Tringe, S. G. et al. (2010). Targeted Metagenomics and Ecology of Globally Important Uncultured Eukaryotic Phytoplankton. *Proceedings of the National Academy of Sciences, 107,* 14679-14684. https://doi.org/10.1073/pnas.1001665107

DHN-Diretoria de Hidrografia e Navegação (2019). *Tábuas das marés*. https://www.marinha.mil.br/chm/dados-do-segnav-publicacoes/tabuas-das-mares

Fofonoff, P., & Millard Jr., R. C. (1983). *Algorithms for Computation of Fundamental Properties of Seawater*. UNESCO, Technical Papers in Marine Science, 44.

Furlong, E. T., & Carpenter, R. (1988). Pigment Preservation and Remineralization in Oxic Coastal Marine Sediments. *Geochimica et Cosmochimica Acta, 52,* 87-99. https://doi.org/10.1016/0016-7037(88)90058-0

Giovanardi, F., & Vollenweider, R. A. (2004). Trophic Conditions of Marine Coastal Waters: Experience in Applying the Trophic Index TRIX to Two Areas of the Adriatic and Tyrrhenian Seas. *Journal of Limnology, 63,* 199-218. https://doi.org/10.4081/jlimnol.2004.199

Gogoi, P., Das, S. K., Jana, C., Das, B. K., Saha, A., Ramteke, K. et al. (2024). Assessing the Trophic Status of a Tropical Microtidal Estuary Applying TRIX and Random Forest—A Combined Approach. *Marine Pollution Bulletin, 200,* Article ID: 116126. https://doi.org/10.1016/j.marpolbul.2024.116126

Grasshoff, K., Kremling, K., & Ehrhardt, M. (1983). *Methods of Seawater Analysis* (2nd ed., 419 p.). Verlagie Chemie.

Gypens, N., Lacroix, G., & Lancelot, C. (2007). Causes of Variability in Diatom and Phaeocystis Blooms in Belgian Coastal Waters between 1989 and 2003: A Model Study. *Journal of Sea Research, 57,* 19-35. https://doi.org/10.1016/j.seares.2006.07.004

Hamilton, S. K., Sippel, S. J., & Bunn, S. E. (2005). Separation of Algae from Detritus for Stable Isotope or Ecological Stoichiometry Studies Using Density Fractionation in Colloidal Silica. *Limnology and Oceanography: Methods, 3,* 149-157. https://doi.org/10.4319/lom.2005.3.149

Hansell, D. A., & Carlson, C. C. (2002). *Biogeochemistry of Marine Dissolved Organic Matter* (774 p.). Academic Press.

Harari, J., França, C. A. S., & Camargo, R. (2008). Perspectives on Integrated Coastal Zone Management in South America. In R. Neves, J. Baretta, & M. Mateus (Eds.), *Climatology and Hydrography of Santos Estuary* (pp. 147-160). IST Press.

INMET (2019). *Portal INMET*. https://portal.inmet.gov.br/

Jeffrey, S. W., & Humphrey, G. F. (1975). New Spectrophotometric Equations for Determining Chlorophylls A, B, C1 and C2 in Higher Plants, Algae and Natural Phytoplankton. *Biochemie und Physiologie der Pflanzen, 167,* 191-194. https://doi.org/10.1016/s0015-3796(17)30778-3

Jenkinson, I. R., Berdalet, E., Chin, W., Denis, M., Ding, H., Duan, J. et al. (2021). The Rôles of Plankton and Neuston Microbial Organic Matter in Climate Regulation. *Journal of Plankton Research, 43*, 801-821. https://doi.org/10.1093/plankt/fbab067

Kimor, B. (1992). The Impact of Eutrophication on Phytoplankton Composition in Coastal Marine Ecosystems. In R. A. Vollenweider, R. Marchetti, & R. Viviani (Eds.), *Marine Coastal Eutrophication* (pp. 871-878). Elsevier. https://doi.org/10.1016/b978-0-444-89990-3.50075-4

Kostadinov, T. S., Siegel, D. A., Maritorena, S., & Guillocheau, N. (2012). Optical Assessment of Particle Size and Composition in the Santa Barbara Channel, California. *Applied Optics, 51,* 3171-3189. https://doi.org/10.1364/ao.51.003171

Lorenzen, C. J. (1965). A Note on the Chlorophyll and Phaeophytin Content of the Chlorophyll Maximum. *Limnology and Oceanography, 10,* 482-483. https://doi.org/10.4319/lo.1965.10.3.0482

Mail Online. https://www.dailymail.co.uk/news/article-2269475/Australia-floods-Entire-towns-lie-submerged-FOUR-FEET-sea-foam-east-coast.html

Masuda, L. S. M., Moser, G. A. O., & Barrera-Alba, J. J. (2011). Variação temporal do microfitoplâncton no Canal Estuarino de Santos (SP). *Brazilian Journal of Aquatic Science and Technology, 15,* 79-93. https://doi.org/10.14210/bjast.v15n1.p79-93

Moser, G. A. O., Gianesella, S. M. F., Alba, J. J. B., Bérgamo, A. L., Saldanha-Corrêa, F. M. P., Miranda, L. B. d. et al. (2005). Instantaneous Transport of Salt, Nutrients, Suspended Matter and Chlorophyll-A in the Tropical Estuarine System of Santos. *Brazilian Journal of Oceanography, 53,* 115-127. https://doi.org/10.1590/s1679-87592005000200003

Moser, G., Ciotti, A., Giannini, M., Tonini, R., & Harari, J. (2012). Changes in Phytoplankton Composition in Response to Tides, Wind-Induced Mixing Conditions, and Freshwater Outflows in an Urbanised Estuarine Complex. *Brazilian Journal of Biology, 72,* 97-111. https://doi.org/10.1590/s1519-69842012000100012

Nunes, L. H. (1990). *Impacto pluvial na serra do paranapiacaba e baixada santista*. PhD Thesis, Universidade de São Paulo.

Oliveira, A., Duarte, J., Silva, A., & Taborda, R. (2014). Dark Grey Sea foam Formation in the "Norte" Beach (Nazaré). In *3as Jornadas de Engenharia Hidrográfica* (pp. 321-326).

Oviatt, C., Lane, P., French, F., & Donagha, P. (1989). Phytoplankton Species and Abundance in Response to Eutrophication in Coastal Marine Mesocosms. *Journal of Plankton Research, 11,* 1223-1244. https://doi.org/10.1093/plankt/11.6.1223

Phaeocystis Research. http://www.phaeocystis.org/index.html

Rahlff, J., Stolle, C., Giebel, H., Mustaffa, N. I. H., Wurl, O., & P. R. Herlemann, D. (2021). Sea Foams Are Ephemeral Hotspots for Distinctive Bacterial Communities Contrasting Sea-Surface Microlayer and Underlying Surface Water. *FEMS Microbiology Ecology, 97,* fiab035. https://doi.org/10.1093/femsec/fiab035

Redfield, A. C. (1958). The Biological Control of Chemical Factors in the Environment. *American Scientist, 46,* 205-221.

Redfield, A. C., Ketchum, B. H., & Richards, F. A. (1963). The Sea: Ideas and Observations on Progress in the Study of the Seas. In M. N. Hill (Ed.), *The Sea* (2nd ed., pp. 26-77). Wiley.

Santos, A. K. D. dos S., Cutrim, M. V. J., Costa, D. S., Cavalcanti, L. F., Ferreira, F. S., Oliveira, A. L. L. et al. (2021). Algal Blooms and Trophic State in a Tropical Estuary Blocked by a Dam (northeastern Brazil). *Ocean and Coastal Research, 69,* Article No. 21009. https://doi.org/10.1590/2675-2824069.20-006akddss

Seluchi, M., Beu, C., & Andrade, K. M. (2017). Características das Frentes Frias Causadoras de Chuvas Intensas no Leste de Santa Catarina. *Revista Brasileira de Meteorologia, 32,* 25-37. https://doi.org/10.1590/0102-778632120150095

Sharoni, S., & Halevy, I. (2020). Nutrient Ratios in Marine Particulate Organic Matter Are Predicted by the Population Structure of Well-Adapted Phytoplankton. *Science Advances, 6,* eaaw9371. https://doi.org/10.1126/sciadv.aaw9371

Silva, B. R. P. d., Pereira, L. C. C., Vila-Concejo, A., & Costa, R. M. d. (2025). Effects of Rainfall Patterns on the Trophic Conditions of a Near-Pristine Amazon Estuary (Brazil). *Regional Studies in Marine Science, 84,* Article ID: 104102. https://doi.org/10.1016/j.rsma.2025.104102

Silva, L. S., Miranda, B. L., & Castro, B. M. (2001). Relatório do Projeto "Oceanografia da Plataforma Interna de São Sebastião" (OPISS) Subprograma Oceanografia Física. *Relatórios técnicos do Instituto Oceanográfico, 47,* 1-3.

Southward, A. J. (1953). Sea Foam. *Nature, 172,* 1059-1060. https://doi.org/10.1038/1721059b0

Strickland, J. D. H., & Parsons, T. R. (1968). *A Practical Handbook of Seawater Analyses* (311 p.). Bulletin/Fisheries Research Board of Canada.

Sutti, B. O., Chiozzini, V. G., Castro, C. G., & Braga, E. S. (2023). Sinking Particles in the Photic Zone: Relations with Biogeochemical Properties in Different Sectors of the Cananéia-Iguape Estuarine-Lagoon Complex (Cielc)-Brazil. *Ocean and Coastal Research, 71,* 1-35. https://doi.org/10.1590/2675-2824071.22075bos

Tréguer, P., & Le Corre, P. (1975). *Manuel d'analyse des sels nutritifs dans l'eau de mer* (2nd ed.). Université de Bretage Occidentale.

Vollenweider, R. A., Giovanardi, F., Montanari, G., & Rinaldi, A. (1998). Characterization of the Trophic Conditions of Marine Coastal Waters with Special Reference to the NW Adriatic Sea: Proposal for a Trophic Scale, Turbidity and Generalized Water Quality Index. *Environmetrics, 9*, 329-357. https://doi.org/10.1002/(sici)1099-095x(199805/06)9:3<329::aid-env308>3.0.co;2-9

Yacobi, Y. Z., & Ostrovsky, I. (2008). Downward Flux of Organic Matter and Pigments in Lake Kinneret (Israel): Relationships between Phytoplankton and the Material Collected in Sediment Traps. *Journal of Plankton Research, 30,* 1189-1202. https://doi.org/10.1093/plankt/fbn070

Zhang, X., Stavn, R. H., Falster, A. U., Gray, D., & Gould, R. W. (2014). New Insight into Particulate Mineral and Organic Matter in Coastal Ocean Waters through Optical Inversion. *Estuarine, Coastal and Shelf Science, 149,* 1-12. https://doi.org/10.1016/j.ecss.2014.06.003

Zilli, M. T., Carvalho, L. M. V., Liebmann, B., & Silva Dias, M. A. (2016). A Comprehensive Analysis of Trends in Extreme Precipitation over Southeastern Coast of Brazil. *International Journal of Climatology, 37,* 2269-2279. https://doi.org/10.1002/joc.4840